Chapter

Wearable Textile Antennas with High Body-Antenna Isolation: Design, Fabrication, and Characterization Aspects

Nikolay Atanasov, Gabriela Atanasova and Blagovest Atanasov

Abstract

This chapter provides a brief overview of the types of wearable antennas with high body-antenna isolation. The main parameters and characteristics of wearable antennas and their design requirements are discussed. Next, procedures (passive and active) to test the performance of wearable antennas are presented. The electromagnetic properties of the commercially available textiles used as antenna substrates are investigated and summarized here, followed by a more detailed examination of their effects on the performance of wearable antennas with high body-antenna isolation. A trade-off between substrate electromagnetic properties and resonant frequency, bandwidth, radiation efficiency, and maximum gain is presented. Finally, a case study is presented with detailed analyses and investigations of the low-profile all-textile wearable antennas with high body-antenna isolation and low SAR. Their interaction with a semisolid homogeneous human body phantom is discussed. The simulations and experimental results from different (in free-space and on-body) scenarios are presented.

Keywords: wearable antenna, flexible antenna, textile antenna, design requirements, SAR, antenna measurements, antenna performance, human body phantom

1. Introduction

The wearables are identified as 1 of the 10 technologies which will change our lives [1]. They offer attractive solutions in diverse areas including healthcare, education, finance, sport, and entertainment. For example, in the area of the healthcare, wearable devices can collect data (on blood pressure, temperature, heart rate, steps, calories burned, and even glucose levels) in real-time and send this information to nearby node (on-body communication between two wearable devices) or remote station (off-body communication between a wearable device and mobile phone, tablet, or personal computer) using body area networks (BANs). In order to realize remote monitoring and real-time feedback to the user, the wearable device needs to be equipped with a sensor, processor, memory, power unit, transceiver, and an antenna.

The wearable antenna plays a significant role in the overall performance of each wireless wearable device because it determines the reliability of the wireless link and directly influences the energy efficiency and battery life of the device [2, 3]. However, because the wearable antenna operates in a specific environment (on or near to the human body), the effects due to lossy body tissues (as impedance mismatching, radiation-pattern distortion, radiation efficiency reduction) make the design of a wearable antenna a difficult task. Therefore, care is needed in designing antennas for wearable devices [4, 5].

2. Wearable antenna design issues, requirements, measurements, and testing

2.1 Design requirements for wearable antennas

The design of wearable antennas for body-centric communications is discussed in [2–8], and the most important requirements are summarized **Table 1**.

2.2 Design procedure

Generally, in wearable antenna design, electrical, mechanical, and safety requirements should be taken into account. Moreover, to obtain the best antenna performance, the antenna-human interaction needs to be taken into account during the first stage of the wearable antenna design process. As the body is composed of different tissues with different material properties, the choice of a proper body model (called phantom) is critical in ensuring a good trade-off between simulation accuracy and complexity [4]. For the initial design, the simplest and fastest option is to use a homogenous flat phantom of the human body. A detailed review of various types of human body models is presented in [3, 11, 12].

Requirements	
Electrical	• Bandwidth: sufficient to cover the frequency bands over which the wearable device is intended to operate ($\|S11\| \leq -10$ dB within the frequency band of interest in both on-body and free-space operation conditions) • High efficiency: more than 50% in both on-body and free-space operation conditions • Appropriate radiation patterns that reduce the electromagnetic radiation toward the human body
Mechanical	• Low-profile • Lightweight • Compactness • Flexibility • Robust
Safety	• Low specific absorption rates (SAR): below worldwide standard limits (1 g-SAR < 1.6 W/kg [9] and 10 g-SAR < 2 W/kg [10])
Manufacturing	• Low cost in both materials and fabrication • Simple structure for ease fabrication and mass production

Table 1.
General design requirements for wearable antennas.

The selection of materials for the conductive and non-conductive elements of the antenna is also an important factor to consider, especially when the antenna is required to possess characteristics such as low-profile, lightweight, compactness, flexibility, and robust. Hence, flexible, thinner, and low-cost materials should be chosen to make the antenna conformable to the person wearing the wearable device and to meet mechanical and manufacturing requirements. Materials like polymers [3, 13], non-conductive fabrics [4], paper [14], and flex film [5, 6] have been used as the substrates in the existing wearable antennas [3, 15]. The choice of material for the antenna's substrate is a critical factor in the performance of the antenna and is examined in depth in Section 3. After the selection of a suitable material for the antenna substrate, its electromagnetic properties (complex permittivity and permeability and loss tangent) must be characterized via measurements [4]. Several (resonant and non-resonant) methods described in [16] can be used for characterization of the electromagnetic properties of flexible materials. For conductive antenna elements, thinner copper or brass foils, electrically conductive fabrics, threads, or ink can be chosen.

Finally, the impact of wearable antennas on the human body also needs to be considered. To study possible effects on body tissues, we must examine the rate at which energy (W) is deposited in a given volume (V) of tissue with specific density (ρ), as shown in Eq. (1):

$$SAR = \frac{d}{dt}\left(\frac{dW}{\rho dV}\right)\left[\frac{W}{kg}\right] \tag{1}$$

SAR can be also calculated from the electric field (E) within the tissue, as shown in Eq. (2):

$$SAR = \frac{\sigma E^2}{\rho}\left[\frac{W}{kg}\right], \tag{2}$$

where σ is the electrical conductivity of the tissue [S/m].

To control the possibility of high local peaks, the maximum permitted SAR is specified as applying to any 1 g or 10 g of tissue [17].

Therefore, the antenna topology with high body-antenna isolation is required to guarantee satisfactory performance and to reduce the SAR when the antenna is placed on the human body. Several antenna designs with a high degree of isolation between the antenna and human tissues have been reported. These designs use a full ground plane [15, 18], an artificial magnetic conducting surface [19], a reflector [13], an electromagnetic bandgap structure [20], or substrate integrated waveguide techniques [2, 21].

Based on the above requirements, a flexible wearable antenna with a low profile, high radiation efficiency, and low SAR can be developed using the algorithm for numerical design and optimization proposed in [3].

After that, a prototype of the optimized design of the wearable antenna can be fabricated using the methods for fabrication of flexible and wearable antennas presented in [5, 8, 13].

Finally, the antenna designs need to be confirmed by both numerical simulations and experimental measurements, first in free space and after that, when antennas are placed on a human body model.

2.3 Measurements and testing

During the wearable antenna design and development process, measurements of classical parameters that describe the antenna's performance such as reflection

coefficient magnitude (|S11|), bandwidth, gain, radiation efficiency, and radiation patterns need to be performed using passive approaches. In passive antenna measurements, the prototype is connected to the measuring equipment (a network analyzer, signal generator, receiver, or spectrum analyzer) using an external coaxial cable. Moreover, full verification of the antenna design requires more extensive testing, such as flexibility tests (described in [4, 5]) and tests which represent the behavior of the antenna in real working conditions (also called active antenna measurements). In these measurements, a wearable device simulator (or a radio communication test module) is used to set up a connection to the antenna under test, which is embedded into a complete operating wearable device (or connected to a radio communication module) to reproduce real-world behavior. In order to conduct accurate and repeatable measurements, a test (anechoic or reverberation) chamber with a controlled environment is required. The schematic setup for passive (cable-fed) and active testing of antennas in an anechoic and reverberation chamber can be found in [22].

Moreover, different measurement scenarios should be investigated to guarantee optimal antenna performance in a variety of operating conditions: free-space (the antenna is in an isolated test fixture made from foam, placed away from the human body) and on-body scenarios (the antenna is very close to the human body phantom or in direct contact with the phantom).

For wearable applications, the effect of antennas on the human body also must be quantified [8]. The SAR distribution can be measured by the thermographic method (described in [23]) or by a commercial DASY-4 system (presented in [24]).

3. The effect of electromagnetic properties of the substrate materials on the performance of wearable antennas with high body-antenna isolation

The major challenge of designing wearable antennas is to make an antenna that is invisible and unobtrusively integrated inside a garment as well as comfortable and non-hindering for the wearer [7, 25]. The integration of antennas into clothes involves using textile materials as dielectric substrates [7].

The substrate material offers not only ergonomic properties and ease of integration into the users' garments, but it impacts on the antenna performance. Moreover, the thickness of the substrate also influences the overall antenna dimensions [26]. A brief survey on electromagnetic (EM) properties of textile materials used in wearable antennas can be found in [4, 26, 27]. However, little information can be found on the effect of EM properties of the substrate materials on the performance of wearable antennas with body-antenna isolation. The following subsections describe the characterization of the EM properties of textile materials (polar fleece, polyester, polyamide-elastane, cotton, and denim) and their effects on performance (resonant frequency, bandwidth, radiation efficiency, and maximum gain) of wearable antennas with body-antenna isolation.

3.1 Characterization of electromagnetic properties of the textile materials

The EM properties (real (ε') and imaginary (ε'') parts of the relative permittivity and loss tangent ($tan\delta$)) of the textile materials were measured by the cavity perturbation method using a rectangular cavity resonator. This method was chosen because it is well known for extracting EM properties of dielectrics, semiconductors, and magnetic and composite materials [16]. All measurements were performed at 2.564 GHz, at temperature 24 ± 1°C. For each textile material, five readings were

			EM properties			
	Thickness mm	**Material layers**	ε'	ε''	$tan\delta$	**Density g/cm^3**
Polar fleece	1.5	One	1.21831	0.00221	0.00183	0.20
Polyester	0.35	One	1.49797	0.00578	0.00389	1.38
	1.5	Four	1.62022	0.00824	0.00509	
Polyamide-elastane	0.5	One	1.52389	0.03103	0.02040	1.14
	1.5	Three	1.54927	0.02268	0.01463	
Cotton	0.52	One	1.63850	0.10199	0.06218	1.52
	1.5	Three	1.63215	0.08049	0.04930	
Denim	0.5	One	1.86986	0.11786	0.06310	1.54
	1.5	Three	1.87813	0.11166	0.05942	

Table 2.
Parameters of the textile materials and results from measurements of their EM properties.

taken, and the average value is given in **Table 2**. To see how material thickness affects the EM properties, we measured ε' and ε'' of the materials at two thicknesses. The first one corresponds to the thickness of one layer of each material. The second was fixed (1.5 mm) for all textile materials—in this case, three/four layers of each material were assembled by an iron-on hemming strip added in between the martial layers to form a 1.5-mm-thick sample.

From the results presented in **Table 2**, it can be observed that the EM properties of the textile materials show a variation with increasing number of layers in the sample. Moreover, the ε' shows small variations with respect to the sample thickness in comparison to ε'' and $tan\delta$. For all materials are observed that with increasing of the thickness of the textile sample, the real part of relative permittivity increases. The ε' value was found to vary between 1.50 (one layer) and 1.62 (four layers) for polyester and between 1.87 (one layer) to 1.88 (three layers) for denim fabric. Another interesting behavior observed is that ε'' and $tan\delta$ of the polyester increase with increasing number of layers (thickness) of the textile sample, while ε'' and $tan\delta$ of the polyamide-elastane, cotton, and denim decrease. These increases are attributed to the presence of glue (in iron-on hemming strip added in between the martial layers), having a high $tan\delta$ compared to the polyester. Indeed, the use of an interface to assemble the layers, such as glue or an adhesive sheet, can lead to variation in EM properties of the textile materials used in the wearable antenna design.

A comparison of different textile materials at the same thickness (1.5 mm) shows that denim has the highest values of ε', ε'', and $tan\delta$. Moreover, the denim and cotton show higher values of $tan\delta$ than polar fleece, polyester, and polyamide-elastane. The higher values of $tan\delta$ can be related to the fact that these textiles are built up from natural fibers. We conclude that the fabrics made from synthetic fibers (polar fleece, polyester, and polyamide-elastane) have a lower relative permittivity and $tan\delta$ than the fabrics made from natural fibers (cotton and denim).

3.2 Effect of textile substrate electromagnetic property variation on the performance of wearable antennas with body-antenna isolation

Based on the EM properties provided by the above subsection, five textile wearable antennas with high body-antenna isolation were designed using the xFDTD (xFDTD, Remcom Inc., State College, PA, USA), a finite-difference time-domain

(FDTD) method-based simulation software. The configuration of the wearable textile antenna with a substrate from denim fabric is illustrated in **Figure 1a**. It consists of a hexagonal shaped monopole on the top of the substrate and a planar rectangular reflector on the bottom. The antenna is fed by a coplanar waveguide (CPW) feed line. This antenna structure is chosen due to its advantages of light-weight, low-profile, low-cost, and easy fabrication, which satisfies the requirements for wearable antennas presented in **Table 1**.

Then, five antennas were manufactured by a cost-effective and time-saving fabrication technique, as described in [28]. The radiating elements of the antennas were built using a highly conductive woven fabric P1168 (supplied by Adafruit, Italy) with a thickness of 0.08 mm and sheet resistance of 0.05 Ω/sq. **Figure 1b–f** shows the fabricated prototypes of the antennas.

Two scenarios were investigated in this subsection to study the effect of the EM properties of the textile substrate on the antenna performance.

At the first stage, a wearable antenna with a substrate from polar fleece was designed (**Figure 2**) to operate in the 2.4–2.48 GHz industrial scientific and medical (ISM) band. The geometrical dimensions of the monopole, CPW, and reflector

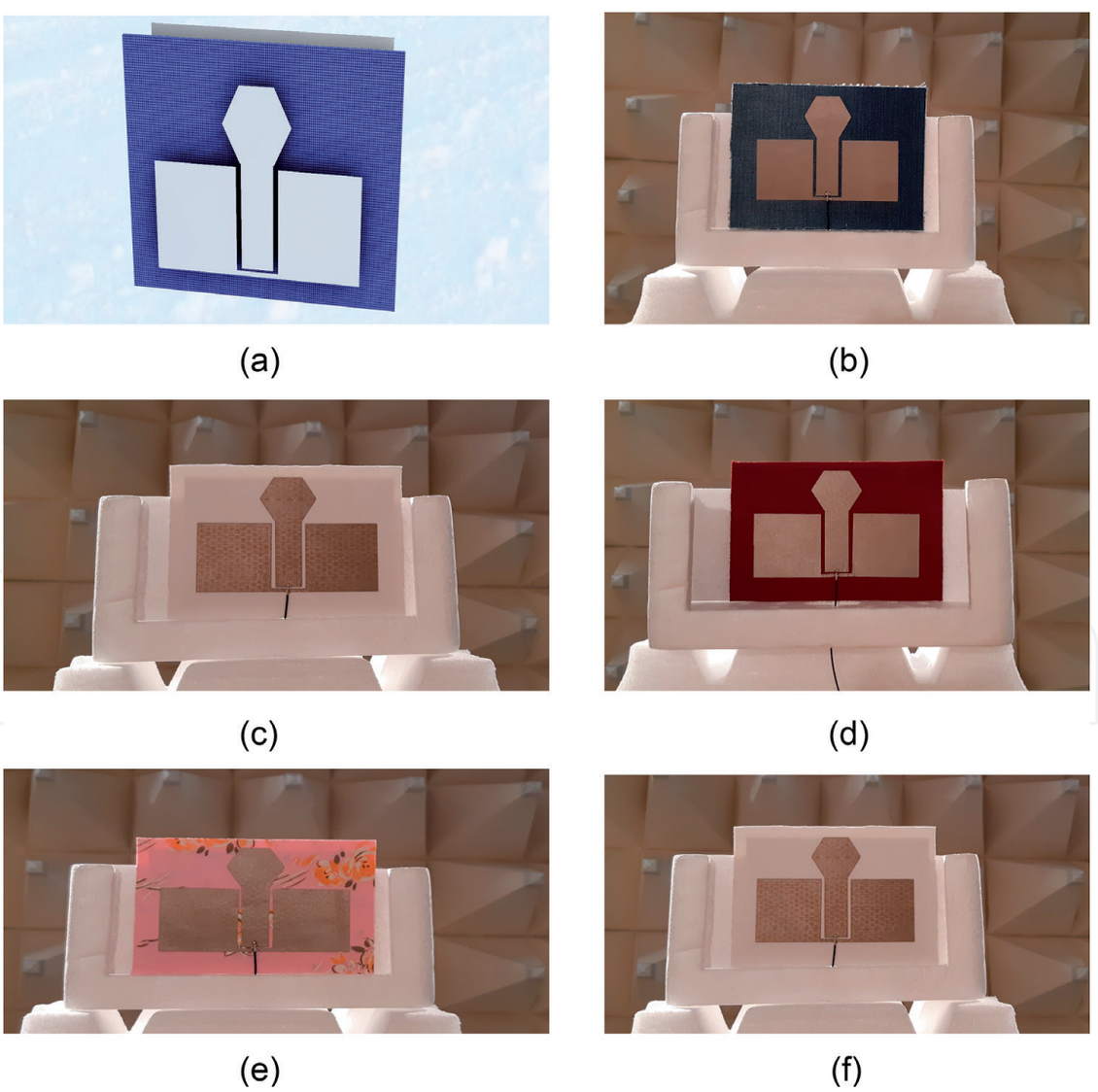

Figure 1.
The (a) 3D numerical model of the textile antenna with a substrate from denim fabric and photographs of the fabricated prototypes, (b) antenna with a denim substrate, (c) antenna with a cotton substrate, (d) antenna with a polyester substrate, (e) antenna with a polyamide-elastane substrate, and (f) antenna with a polar fleece substrate.

were tuned by numerical simulations, following the optimization procedure in [3], to achieve the optimal impedance match, high radiation efficiency, and high front-to-back (FB) ratio at the targeted ISM band. The dimensions of the antenna are listed in **Table 3**.

For comparison purposes, five different numerical models of the wearable antenna with different substrates (from cotton, denim, polyester, polyamide-elastane, air) and geometrical dimensions as that of the antenna with a substrate from polar fleece were built. The resonant frequency of the antennas calculated by the simulations is compared in **Figure 3a**.

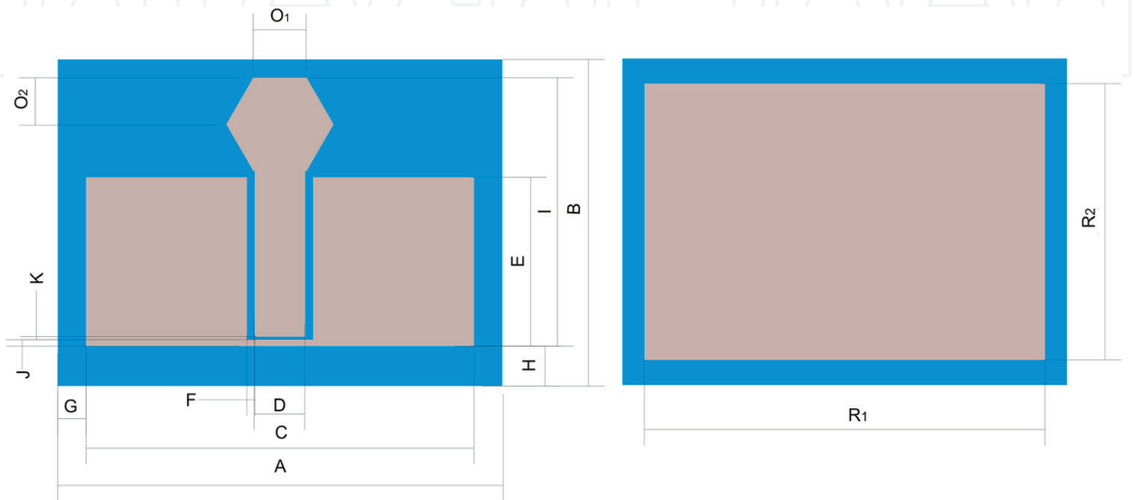

Figure 2.
Configuration of the wearable antenna.

	Antenna with an air-filled substrate	Antenna with a polyester substrate	Antenna with a polyamide-elastane substrate	Antenna with a cotton substrate	Antenna with a denim substrate	Antenna with a polar fleece substrate
A	141.0	141.0	141.0	141.0	141.0	141.0
B	103.5	103.5	103.5	103.5	103.5	103.5
C	134.0	110.0	112.0	109.0	103.0	123.0
D	21.0	21.0	21.0	21.0	21.0	21.0
E	59.0	47.0	48.0	46.5	43.5	53.5
F	2.5	2.5	2.5	2.5	2.5	2.5
G	—	16.5	15.5	17.0	20.0	10.0
H	—	16.5	15.5	17.0	20.0	10.0
I	90.0	78.0	79.0	77.5	74.5	84.5
J	2.0	2.0	2.0	2.0	2.0	2.0
K	1.0	1.0	1.0	1.0	1.0	1.0
O_1	17.0	17.0	17.0	17.0	17.0	17.0
O_2	17.0	17.0	17.0	17.0	17.0	17.0
R_1	138.0	127.0	127.0	127.0	127.0	127.0
R_2	93.0	87.5	87.5	87.5	87.5	87.5

Table 3.
The geometrical dimensions of the optimized antennas.

As expected, the antenna with a substrate filled by air ($\varepsilon_r' = 1$) shows the highest value of resonant frequency (f_{r0}) of 2.66 GHz. For antennas with substrates from textile materials, the resonant frequency drops (to a value of $f_{r0}/\sqrt{\varepsilon_r'}$) as the ε_r' increase, because more energy is coupled into guided waves inside the substrate.

Next, the effects of the EM properties of the textile substrate on the bandwidth were evaluated and illustrated in **Figure 3b–d**. The bandwidth of all antennas was defined for |S11| = −10 dB. **Figure 3b** shows the bandwidth as a function of the ε_r' of the textile substrates. It is observed that the ε_r' of the textile substrate does not strongly influence the bandwidth. This effect can be attributed to the fact that ε_r' of the textiles are within the range between 1.2 and 1.9 (see **Table 2**). Moreover, the bandwidth increases with an increase in the ε_r'' (see **Figure 3c**).

As shown in **Figure 3d**, the antennas with a substrate from denim and cotton have the largest bandwidth (150.5 MHz) because these two fabrics have the highest values of ε_r'' and $tan\delta$ at a thickness of 1.5 mm (see **Table 2**) and, thus, the highest dielectric losses. As expected, a decline in the bandwidth is observed as the dielectric loss of the substrate is decreased. Hence, it can be concluded that the antenna bandwidth is proportional to the textile substrate loss tangent.

From the results mentioned here, it also can be concluded that fabrics made from synthetic fibers (polar fleece, polyamide-elastane, polyester) exhibit a narrow bandwidth compared to the fabrics made from natural fibers (cotton and denim).

Moreover, it is well known that the bandwidth and radiation efficiency not only are determined by the substrate's EM properties and thickness but

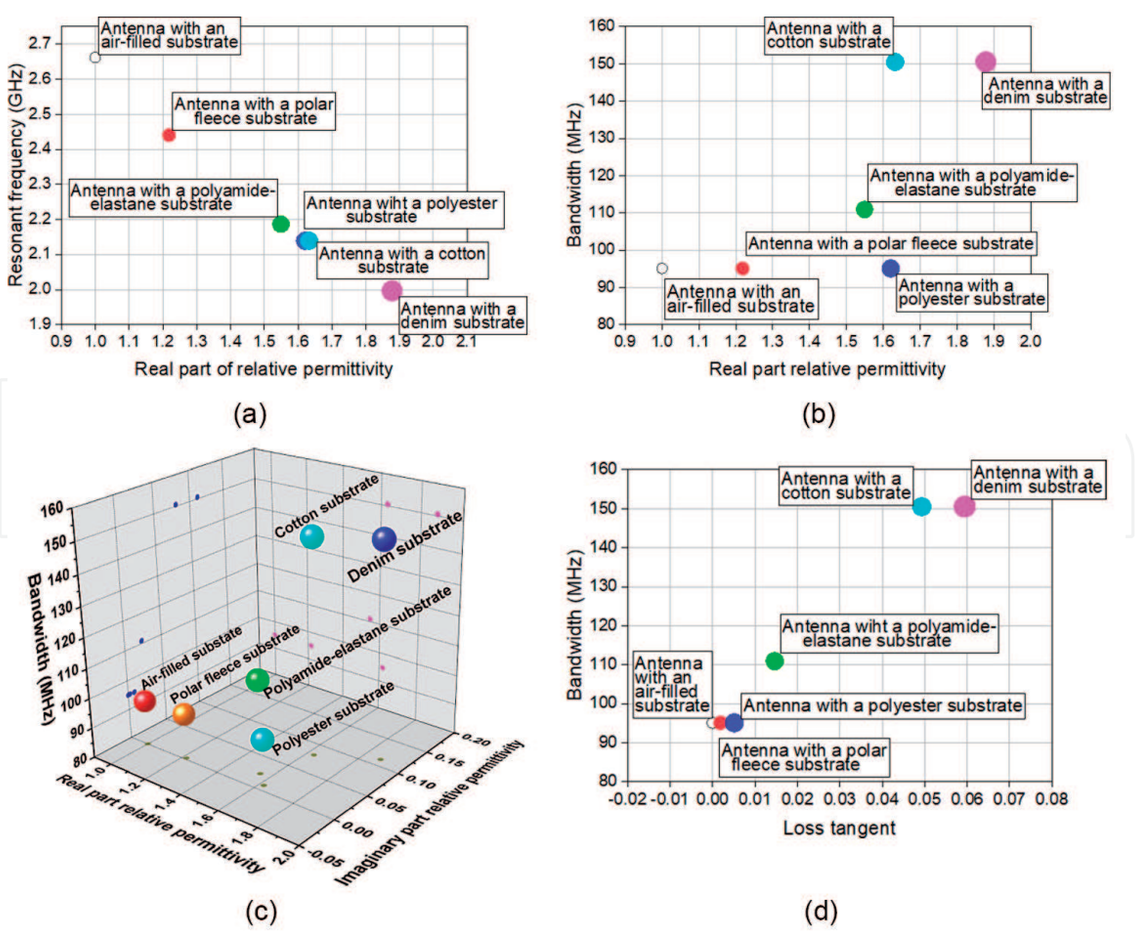

Figure 3.
Variation of (a) resonant frequencies and (b) bandwidths with the ε_r', (c) bandwidths with ε_r' and ε_r'', and (d) bandwidths with the loss tangent of the textile substrates used in wearable antennas with the same geometrical dimensions.

also depend on the size of the antenna radiating elements and matching. Consequently, it is necessary to know the effect of the EM properties of the textile materials on antenna performance when antenna elements are optimized. For this reason, in the second scenario, the structure of the antennas with a polyester, polyamide-elastane, denim, cotton, and air-filled substrate was optimized for the maximum impedance bandwidth, radiation efficiency, and high FB ratio at the 2.4–2.48 GHz frequency band. The optimized dimensions are listed in **Table 3**.

To illustrate the effects of textile materials on the antenna performance, the optimized antenna designs considered in **Table 3** were evaluated in the free space and when placed on a flat phantom. First, a flat homogeneous semisolid phantom of the human body with dimensions 265 × 50 × 350 mm to emulate 2/3 muscle tissue was fabricated accordingly to the recipe and technique described in [29]. After the phantom mixture had solidified, EM properties were measured at 2.564 GHz: ε_r' =40.805 and σ = 2.33 S/m. Next, a numerical flat homogeneous human body model (called flat phantom) with dimensions and EM properties as those of the fabricated phantom was developed. The fabricated experimental and numerical phantoms used in this chapter are illustrated in **Figure 4**.

The results from numerical simulations in both free space and on-body are presented in **Figures 5–9**. **Figure 5** displays the bandwidth as a function of the loss tangent of the textile substrate. As seen in these plots, the bandwidth remains unchanged in both free space (**Figure 5a**) and on-body (**Figure 5b**) for the antennas with a polyester, cotton, and denim substrate. A slight bandwidth broadening is observed when the optimized antennas with an air-filled, polar fleece and polyamide-elastane substrate are placed on the flat phantom. The reason for this effect

Figure 4.
Flat phantom and the antenna with a denim substrate: (a) a photograph and (b) numerical models.

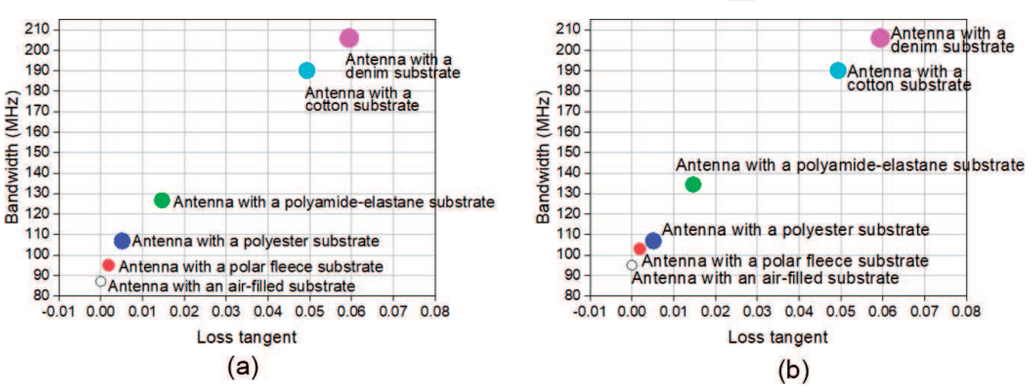

Figure 5.
Variation of the bandwidth with the loss tangent of the textile substrates used in optimized wearable antennas with geometrical dimensions listed in **Table 3**, *in both (a) free space and (b) on-body.*

is that the real part of the relative permittivity of these materials (at a thickness of 1.5 mm, see **Table 2**) is between 1 and 1.55. Consequently, we can conclude that the performance of the wearable antennas with substrates made from fabrics with real part of the relative permittivity small than 1.6 will be influent from the proximity of the human body.

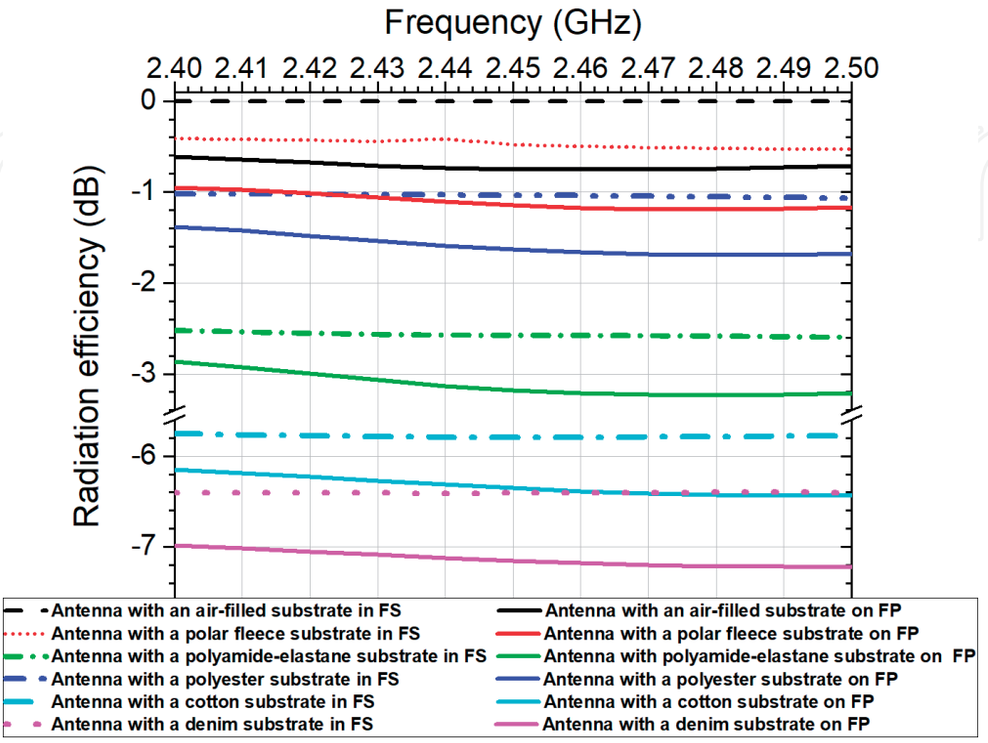

Figure 6.
Simulated radiation efficiency curves versus frequency of the wearable antennas: in the free space (FS) and on the flat phantom (FP).

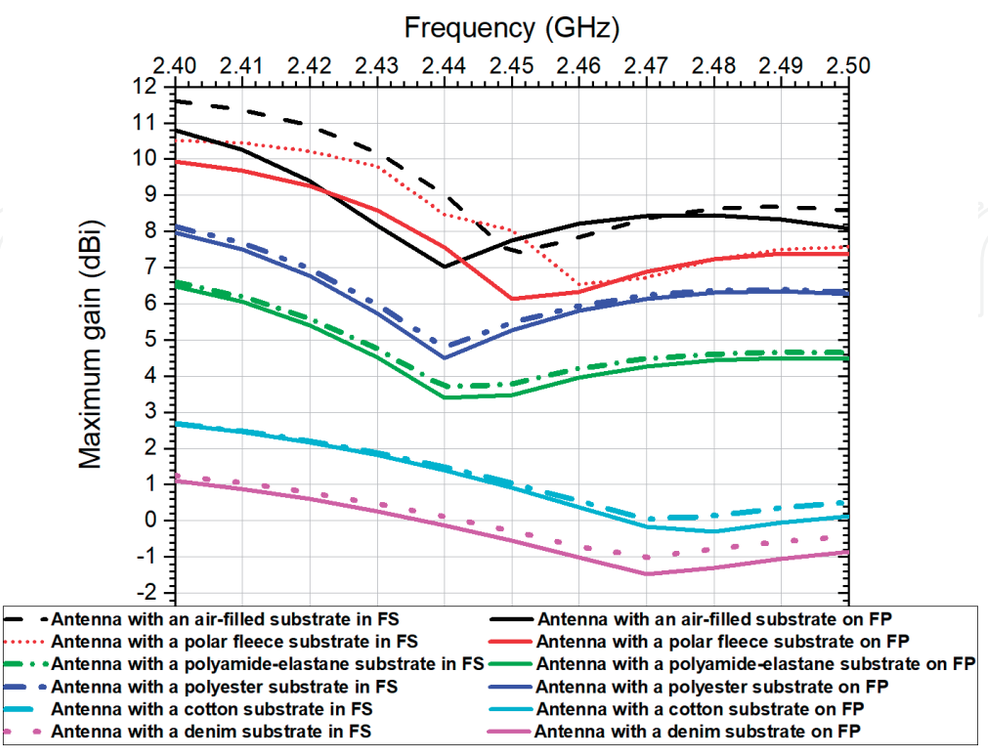

Figure 7.
Simulated maximum gain curves versus frequency of the wearable antennas: in the free space (FS) and on the flat phantom (FP).

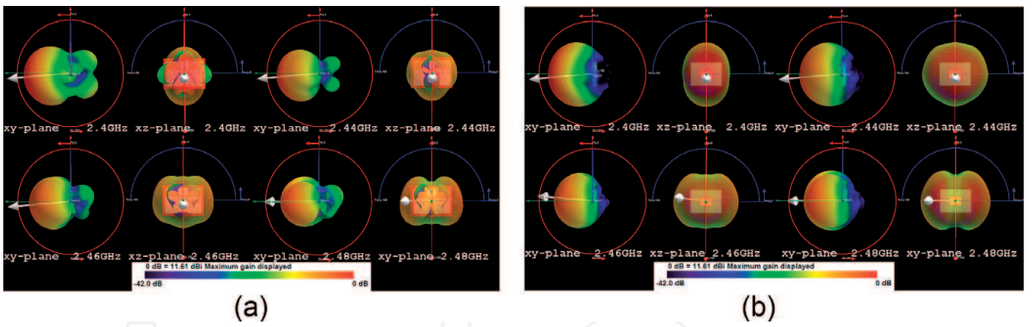

Figure 8.
Simulated three-dimensional radiation patterns at 2.4, 2.44, 2.46, and 2.48 GHz for the antenna with a polar fleece substrate (a) in the free space and (b) on the flat phantom.

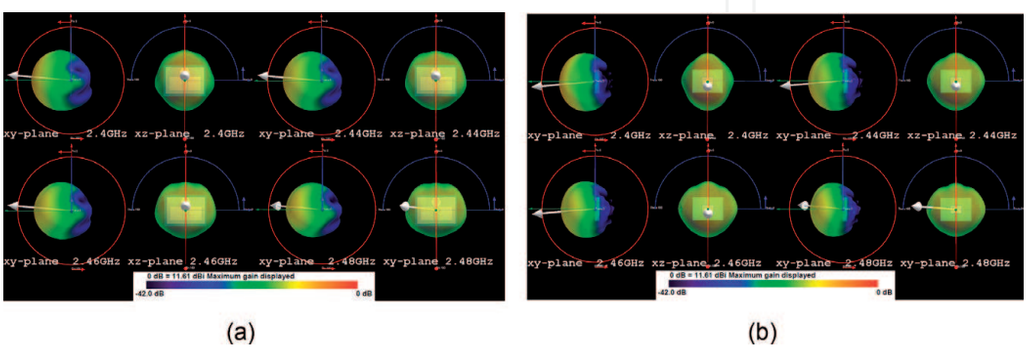

Figure 9.
Simulated three-dimensional radiation patterns at 2.4, 2.44, 2.46, and 2.48 GHz for the antenna with a denim substrate (a) in the free space and (b) on the flat phantom.

A comparison between the simulated radiation efficiency of the antennas is displayed in **Figure 6**. The radiation efficiency is defined as the ratio of the power radiated from the antenna to the net input power, which is the radiated power plus material losses [30]. The comparison shows that the antennas with polar fleece, polyester, and polyamide-elastane substrates achieve a much better radiation efficiency than the antennas with substrates from cotton and denim. These differences are attributed to the fact that fabrics made from synthetic fibers have lower $tan\delta$ than the fabrics made from natural fibers. Moreover, it can be observed that the simulated radiation efficiency of all antennas is quite stable in the target frequency range, on both the free space and on-body.

From the results presented in **Figure 6**, a slight reduction of radiation efficiency when the antennas are placed on the flat phantom (FP) also can be observed. For example, across the operating band, the radiation efficiency of the antenna with a substrate from polar fleece is estimated to be −0.47 dB (90%) in the free space and − 1.1 dB (78%) when it is placed on the phantom.

The maximum gain of the optimized antennas was also evaluated and illustrated in **Figure 7**. As seen, in the target frequency band, the gain varies between 11 and 7 dBi (for the antenna with a polar fleece substrate) and between 1 and −1 dBi (for the antenna with a denim substrate). The variation in maximum gain values is related to the maximum directivity (see **Figure 8**) and is primarily due to the coupling between radiating elements and the reflector. The gain difference between the antennas with substrates from fabrics made with synthetic fibers and fabrics made with natural fibers can be associated with the differences in their radiation efficiency (see **Figure 6**). Moreover, the maximum gains of the antennas mounted directly on the flat phantom are not strongly affected by the phantom (human body).

Figures 8 and **9** compare the three-dimensional (3D) radiation patterns of the optimized wearable antennas with polar fleece and denim substrates, at 2.4, 2.44, 2.46, and 2.48 GHz. These frequencies approximately correspond to the lower, middle, and upper end of the 2.45 GHz ISM band. As shown in **Figures 8** and **9**, the radiation is unidirectional for the antennas at all frequencies. Three-dimensional patterns show that a small amount of the energy is radiated in the backward direction (i.e., behind the antenna) into the human body. Moreover, it can be observed that in the free space, the Eφ is the dominant field component at 2.4, 2.44, and 2.46 GHz for the antennas. At 2.48 GHz, the Eθ is the dominant field component for these antennas. Hence, we observe that the directivity is decreased with increasing frequency because more energy is radiated in θ direction.

As can be seen in the figures, the radiation patterns of the antennas are not significantly modified by the presence of the flat phantom.

Figure 10 shows FB radio as a function of frequency both in free space and on a phantom. As seen, in the target frequency band, the FB ratios vary between 12 and 33 dB in the free space and between 18 and 36 dB on the phantom, depending on the antenna's substrate. A FB ratio of about 30 dB is achieved for the antennas with denim and cotton substrates in the free space, in the frequency band of 2.4–2.46 GHz, indicating a small amount of radiation behind the antenna.

As seen in **Figure 10**, both antennas with polyester and polyamide-elastane substrates have FB ratio better than 17 dB in the free space and better than 23 dB on the phantom. Moreover, the antennas with cotton, polyester, polyamide-elastane, and denim preserve their FB ratios when placed directly on the flat phantom. In the case of the antennas with polar fleece and air-filled substrate, we see a FB ratio between 12 and 20 dB in the free space and between 25 and 35 dB when antennas are placed directly on the flat phantom; this will result in an increase in SAR values (see **Figure 11**). Comparing the FB ratios of the antennas, it can be concluded that the cotton and denim textile substrates improve FB ratio of the antenna.

3.3 Effect of wearable antennas with textile substrates on the human body

Because the wearable textile antennas are designed to operate near to the human body, in this subsection, we investigate the effects of these antennas on the human

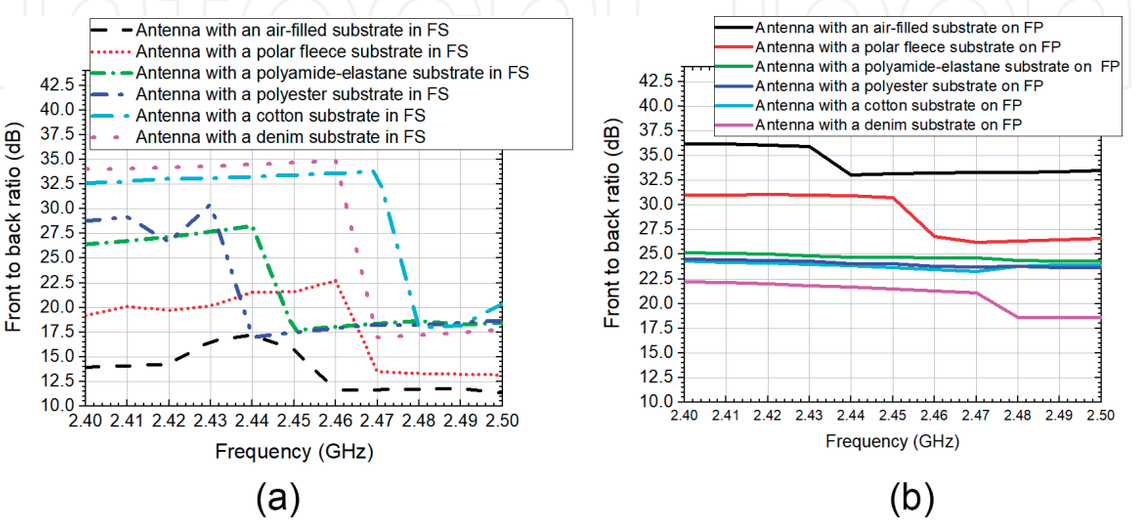

Figure 10.
Simulated front-to-back radio as a function of frequency in both (a) free space and (b) on phantom.

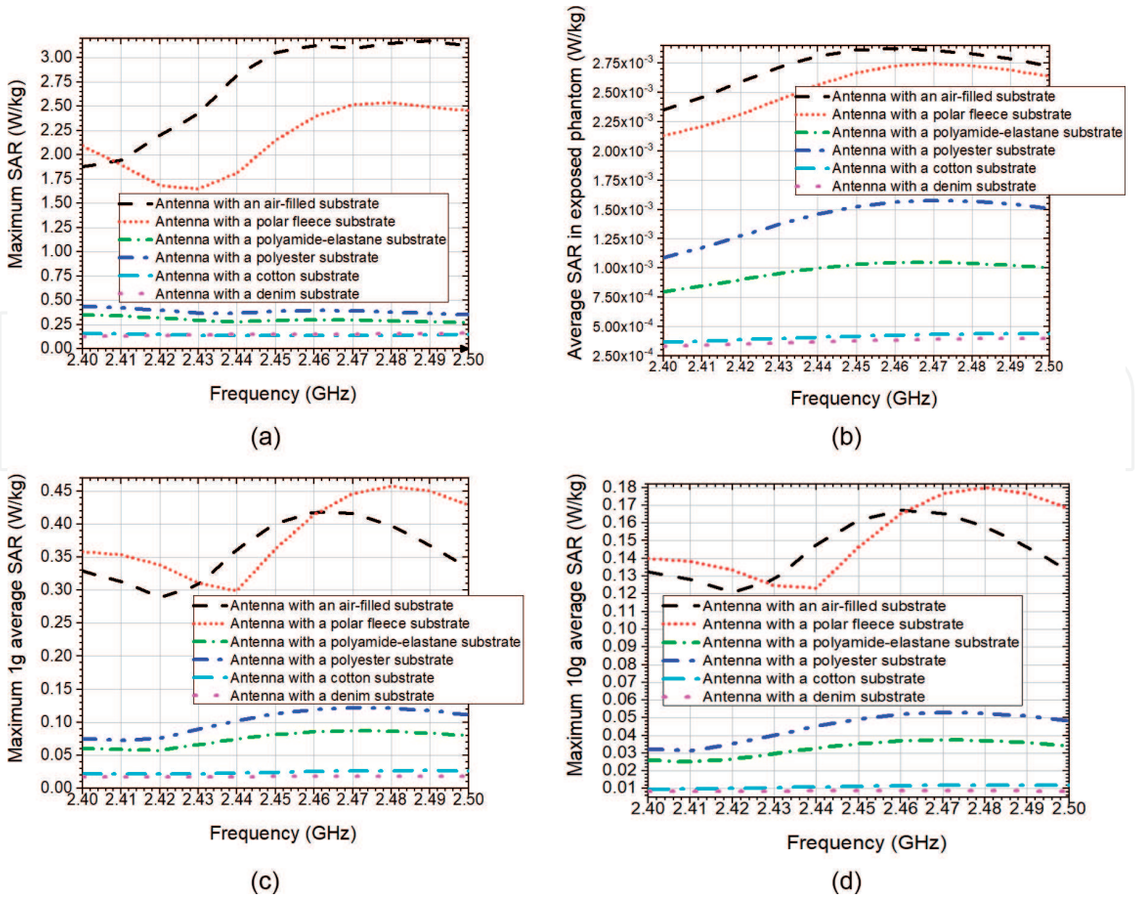

Figure 11.
SAR as a function of frequency (a) the maximum local SAR, (b) average SAR in exposed flat phantom, (c) maximum 1 g average SAR and (d) maximum 10 g average SAR.

body by evaluating the SAR. For these computations, each antenna was placed directly on the numerical flat homogeneous human body model as presented in **Figure 4b**.

Figure 11a–d shows the maximum local SAR, average SAR in exposed flat phantom, and maximum 1 g and 10 g average SAR as a function of frequency. The results presented in **Figure 11a–d** were normalized to net input power of 100 mW. As can be seen in the figures, the SAR values from the antennas with air-filled and polar fleece substrates are higher than the SAR from the other antennas. Moreover, the maximum 10 g average SAR is 0.18 (antenna with a polar fleece substrate) and between 0.04 and 0.1 W/kg for the rest of the antennas. Therefore, maximum 10 g average SAR for all antennas is 90% lower than the specification required by the ICNIRP [10] and also smaller than most of the previously proposed wearable textile antennas.

The differences in SAR distributions between the antennas are illustrated in **Figure 12a–f**. For all antennas, the peak SAR in the phantom occurs in the region near the antenna edges. Moreover, the SAR distribution of the antenna with a polar fleece substrate is similar to that of the antenna with an air-filled substrate. Also, the SAR distribution of the antennas with a substrate from cotton and denim is quite similar.

SAR values presented in **Figure 12** were averaged over a volume of 0.125 mm^3 containing a mass of 0.14575 mg.

Measurements were carried out to validate the simulations. **Figure 13** shows the simulated and measured reflection coefficient magnitudes of the wearable antennas in the free space and on the phantom. A small difference between

simulated and measured results was observed. This difference can be attributed to fabrication and assembly inaccuracies (due to the manual assembly).

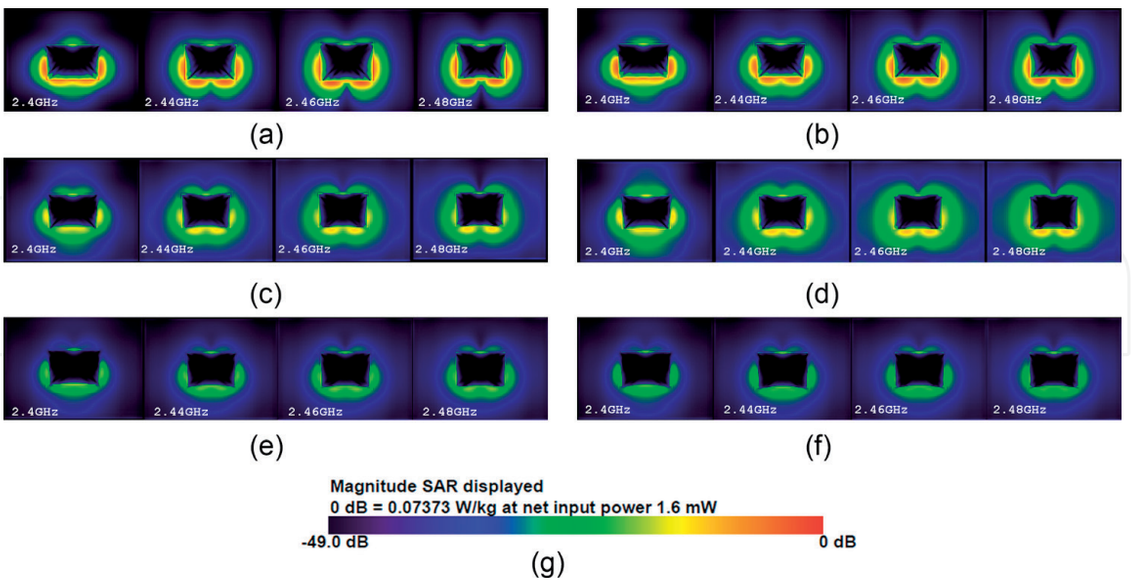

Figure 12.
SAR distributions at 2.4, 2.44, 2.46, and 2.48 GHz for the antenna with (a) an air-filled substrate, (b) a polar fleece substrate, (c) a polyamide-elastane substrate, (d) a polyester substrate, (e) a cotton substrate, (f) a denim substrate, and (g) scale.

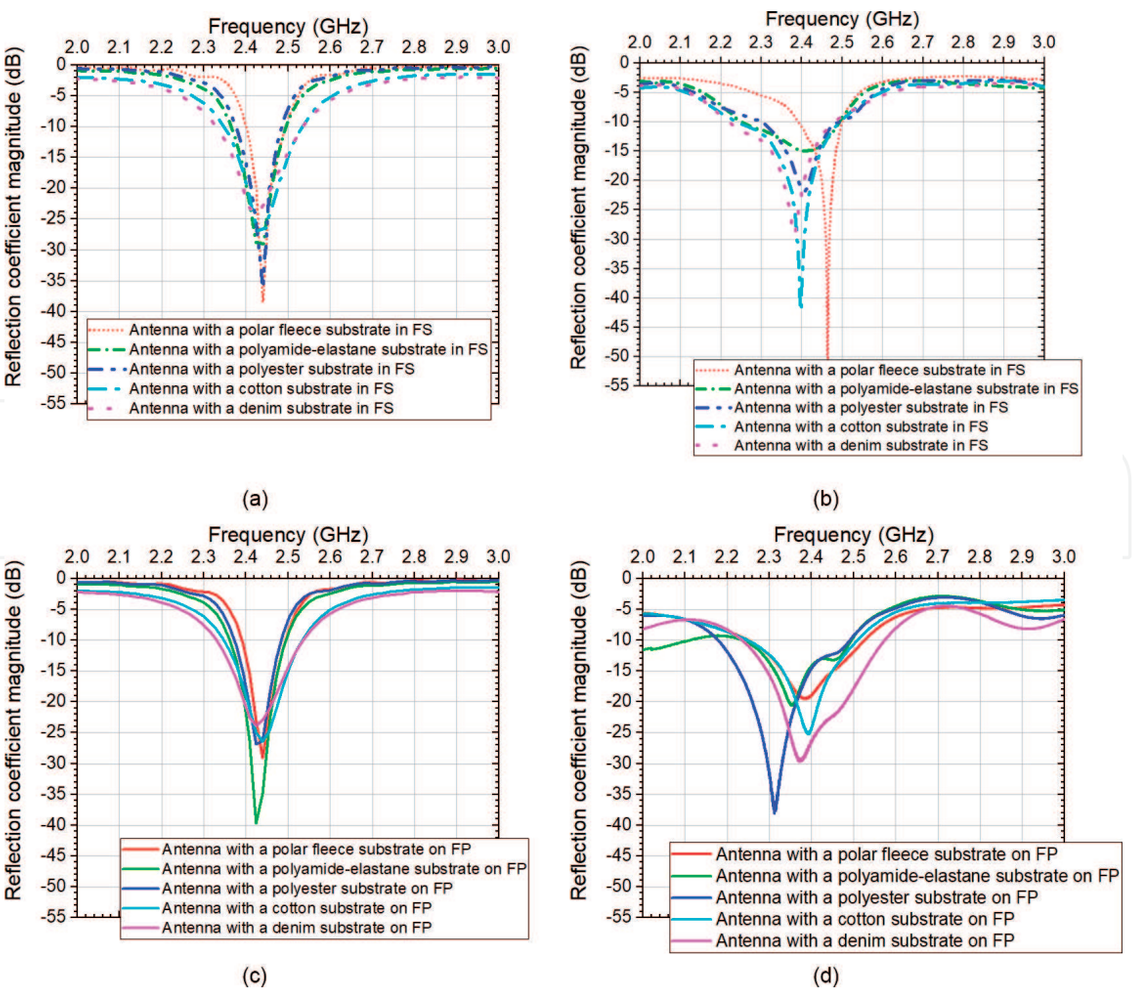

Figure 13.
|S11| curves versus frequency (a) simulated in the free space, (b) measured in the free space, (c) simulated on the phantom, and (d) measured on the phantom.

Moreover, the coaxial cable and U. FL connector were not integrated into the FDTD simulations, which also lead to a difference between the simulations and measurements.

We can conclude that the antennas demonstrate stable performance on both in the free space and when placed directly on the flat phantom.

4. Conclusions

In this chapter, the main parameters and characteristics of wearable antennas and their design requirements have been presented. The electromagnetic properties of the textile substrates also have been examined. From the results mentioned here, it is concluded that fabrics made from synthetic fibers (polar fleece, polyamide-elastane, polyester) have a lower relative permittivity and $tan\delta$ than the fabrics made from natural fibers (cotton and denim). It is interesting to note that for the wearable antennas with high body-antenna isolation, an increase in the real part of the relative permittivity of the textile substrate had minimal impact on the antenna bandwidth. Moreover, the loss tangent of the textile substrate affects the wearable antenna's bandwidth and radiation efficiency: the higher the loss tangent, the broader the bandwidth and the lower the radiation efficiency. We conclude that the EM properties (ε_r', ε_r'', $tan\delta$), thickness of the textile substrate and radiating element geometry, play an important role in determining the antenna's performance and need to be taken into account when designing a wearable antenna with high body-antenna isolation.

Five low-profile all-textile antennas with high body-antenna isolation have been presented. The in-depth performance evaluations on both in the free space and on the flat phantom of these antennas indicate that they cover 2.45 GHz ISM band and the maximum 10 g average SAR for all antennas is 90% lower than the specification.

Acknowledgements

The author would like to acknowledge the Bulgarian National Science Fund, Ministry of Education and Science, Bulgaria, for the support through a grant № KP-06-H27/11 from 11 December 2018 "Antenna technology for wearable devices in the future communication networks."

Author details

Nikolay Atanasov[1,2*], Gabriela Atanasova[1] and Blagovest Atanasov[3]

1 South-West University "Neofit Rilski", Blagoevgrad, Bulgaria

2 Electromagnetic Compatibility Laboratory, Bulgarian Institute of Metrology, Sofia, Bulgaria

3 91 German Language High School "Prof. Konstantin Galabov", Sofia, Bulgaria

*Address all correspondence to: natanasov@windowslive.com; natanasov@swu.bg

References

[1] European Commission Directorate-General for Communications Networks, Content and Technology, Smart Wearables: Reflection and Orientation Paper. Digital Industry Competitive Electronics Industry, Brussels; 2016

[2] Agneessens S. Coupled eighth-mode substrate integrated waveguide antenna: Small and wideband with high-body antenna isolation. IEEE Access. 2017;**6**:1595-1602. DOI: 10.1109/ACCESS.2017.2779563

[3] Al-Sehemi A, Al-Ghamdi A, Dishovsky N, Atanasov N, Atanasova G. Wearable antennas for body-centric communications: Design and characterization aspects. Applied Computational Electromagnetics Society Journal. 2019;**34**:1172-1181

[4] Werner D, Jiang Z-H. Electromagnetics of Body-Area Networks, Antennas, Propagations and RF Systems. 1st ed. Hoboken: John Wiley & Sons, Inc.; 2016. pp. 1-59

[5] Khaleel R, Al-Rizzo H, Ayman I. Design, fabrication, and testing of flexible antennas. In: Kischk A, editor. Advancement in Microstrip Antennas with Recent Applications. 1st ed. London: IntechOpen; 2013. pp. 365-383. DOI: 10.5772/50841

[6] Raad H, Abbosh A, Al-Rizzo H, Rucker D. Flexible and compact AMC based antenna for telemedicine applications. IEEE Transactions on Antennas and Propagation. 2013;**61**(2):524-531

[7] Nepa P, Rogier H. Wearable antennas for off-body radio links at VHF and UHF bands: Challenges, state-of-the-art, and future trends below 1 GHz. IEEE Antennas and Propagation Magazine. 2015;**57**(5):30-52. DOI: 10.1109/MAP.2015.2472374

[8] Khaleel H, editor. Innovations in Wearable and Flexible Antennas. 1st ed. Southampton: WIT press; 2015. pp. 8-54. ISBN: 978-1-84-564-986-9

[9] IEEE Standards Coordinating Committee. IEEE for safety levels with respect to human exposure to radio frequency electromagnetic fields, 3 kHz to 300 GHz. IEEE Standards. 2005;**C95**:1

[10] ICNIRP. Guidelines for limiting exposure to time-varying electric, magnetic, and electromagnetic fields (up to 300 GHz). Health Physics. 1998;**74**:494-522

[11] Pellegrini A, Brizzi A, Zhang L, Ali K, Hao Y, Wu X, et al. Antennas and propagation for body-centric wireless communications at millimeter-wave frequencies: A review [wireless corner]. IEEE Antennas and Propagation Magazine. 2013;**55**(4):262-287. DOI: 10.1109/MAP.2013.6645205

[12] Björninen T. Comparison of three body models of different complexities in modelling of equalsized dipole and folded dipole wearable passive UHF RFID tags. Applied Computational Electromagnetics Society Journal. 2018;**33**:706-709

[13] Al-Sehemi A, Al-Ghamdi A, Dishovsky N, Atanasov N, Atanasova G. Design and performance analysis of dual-band wearable compact low-profile antenna for body-centric wireless communications. International Journal of Microwave and Wireless Technologies. 2018;**10**:1175-1185

[14] Anagnostou D, Gheethan A, Amert A, White K. A direct-write printed antenna on paper-based organic substrate for flexible displays and WLAN applications. Journal of Display Technology. 2010;**6**(11):558-564. DOI: 10.1109/JDT.2010.2045474

[15] Simorangkir R, Kiourti A, Esselle K. UWB wearable antenna with full ground plane based on PDMS-embedded conductive fabric. IEEE Antennas and Wireless Propagation Letters. 2018;**17**(3):493-496. DOI: 1109/LAWP.2018.2797251

[16] Chen L, Ong C, Neo C, Varadan VV, Varadan KV. Microwave Electronics: Measurement and Materials Characterization. 1st ed. Chichester: John Wiley & Sons, Inc.; 2004. pp. 37-141

[17] Chen Z-N. Antennas for portable devices. 1st ed. Chichester: John Wiley & Sons, Inc.; 2007. pp. 20-40. ISBN 978-0-470-03073-8

[18] Abbas S, Zahra H, Hashmi R, Esselle K, Volakis J. Compact on-body antennas for wearable communication systems. In: International Workshop on Antenna Technology (iWAT); 3-6 March 2019. Miami, Florida, United Sates of Amerika: IEEE; 2019

[19] Jiang Z-N, Brocker D, Sieber P, Werner D. A compact, low-profile metasurface-enabled antenna for wearable medical body-area network devices. IEEE Transactions on Antennas and Propagation. 2014;**62**(8):4021-4030. DOI: 10.1109/TAP.2014.2327650

[20] Ashyap A, Abidin Z, Dahlan S, Majid H, Kamarudin M, Alomainy A, et al. Highly efficient wearable CPW antenna enabled by EBG-FSS structure for medical body area network applications. IEEE Access. 2018;**6**:77529-77541. DOI: 10.1109/ACCESS.2018.2883379

[21] Agneessens S, Lemey S, Rogier H, Vervust T, Vanfleteren J. Applying QMSIW technique in textile for compact wearable design and high body-antenna isolation. In: IEEE International Symposium an Antennas and Propagation & USNC/URSI Radio Science Meeting; 19-24 July 2015. Vancouver, BC, Canada; 2015

[22] Anguera J, Andújar A, Huynh M-C, Orlenius C, Picher C, Puente C. Advances in antenna technology for wireless handheld devices. International Journal of Antennas and Propagation. 2012;**2013**:1-25

[23] Al-Sehemi A, Al-Ghamdi A, Dishovsky N, Atanasov N, Atanasova G. Flexible and small wearable antenna for wireless body area network applications. Journal of Electromagnetic Waves and Applications. 2017;**31**:1063-1082. DOI: 10.1080/09205071.2017.1336492

[24] Schmid T, Egger O, Kuster N. Automated E-field scanning system for dosimetric assessments. IEEE Transactions on Microwave Theory and Techniques. 1996;**44**(1):105-113. DOI: 10.1109/22.481392

[25] Corchia L, Monti G, Tarricone L. Wearable antennas: Nontextile versus fully textile solutions. IEEE Antennas and Propagation Magazine. 2019;**61**(2):71-83. DOI: 10.1109/MAP.2019.2895665

[26] Salvado R, Loss C, Gonçalves R, Pinho P. Textile materials for the design of wearable antennas: A survey. Sensors. 2012;**12**:15841-15857. DOI: 10.3390/s121115841

[27] Velez F, Miyandoab F, editors. Wearable Technologies and Wireless Body Sensor Networks for Healthcare. 1st ed. London: The Institution of Engineering and Technology; 2019. pp. 147-183. ISBN:978-1-78561-217-6

[28] Atanasov N, Atanasova G, Stefanov A, Nedialkov I. A wearable, low-profile, fractal monopole antenna integrated with reflector for enhancing antenna performance and SAR reduction. In: IEEE MTT-S International

Microwave Workshop Series an Advanced Materials and Processes for RF and THz Applications (IMWS-AMP); 16-18 July 2019. Bochum, Germany: IEEE; 2019. pp. 67-69

[29] Yilmaz T, Foster R, Hao Y. Broadband tissue mimicking phantoms and a patch resonator for evaluating noninvasive monitoring of blood glucose levels. IEEE Transactions on Antennas and Propagation. 2014; **62**(6):3064-3075. DOI: 10.1109/TAP.2014.2313139

[30] Elwi T, Al-Rizzo H, Rucker D, Khaleel H. Effects on twisting and bending on the performance of a miniaturized truncated sinusoidal printed circuit antenna for wearable biomedical telemetry devices. AEU - International Journal of Electronics and Communications. 2010;**65**:217-225. DOI: 10.1016/j.aeue.2010.03.008